# Microphysical Parameterization

*Learning Objectives*

Following this lecture, students will be able to:

- Provide a basic description of what parameterizations attempt to represent and how they attempt to represent them in numerical weather prediction models.
- Define and discuss differences between bin, bulk, and Lagrangian microphysical parameterization approaches.
- Describe what is parameterized by single-, double-, and triple-moment microphysical parameterizations.
- Understand the microphysical processes that must be parameterized to adequately represent the evolution and impacts of any given microphysical species in a forecast.
- Recognize how other investigators have designed experiments to test hypotheses relating to how microphysical parameterizations influence a desired forecast element.

*Reference Materials*

The following lecture draws primarily from Chapter 7 of *Parameterization Schemes* by David Stensrud and "An overview of cloud and precipitation microphysics and its parameterization in models," a presentation given by Hugh Morrison at the 2010 WRF Workshop. This lecture also draws a limited amount of information from Morrison et al. (2020, *J. Adv. Model. Earth Sys.*), an excellent modern review of microphysical parameterizations. These references, and the references each work cites, should be referred to for further information.

*A Review of Parameterization Principles*

A model's resolution, which is a function of its grid spacing, defines the minimum length scale that it can resolve. However, no matter the model's resolution, there are important physical processes on smaller scales than those the model can resolve, referred to as the *subgrid-scale*. Examples of such processes include cloud microphysics, deep and shallow cumulus clouds, turbulent vertical mixing, radiative transfer, and exchanges between the atmosphere and the surface. These processes must be **parameterized** by the numerical model.

Physical parameterizations *approximate* subgrid-scale processes and their impacts on the resolved scales as a function of resolved-scale variables. Although guided by theory, parameterizations are largely empirically formulated, with equation structures that have traditionally been prescribed by their developers and tunable parameters determined by fitting

the equations to limited observations or output from models that explicitly resolve the associated physical processes. More recently, parameterizations generated using machine-learning techniques, whether to augment parts of existing parameterizations, emulate existing parameterizations (e.g., to reduce their runtime), or formulate altogether new parameterizations, have begun to be developed and tested.

Parameterized processes are those that are often associated with 'interesting' weather, such as the diurnal cycle and organized convective systems. Uncertainty in numerical approximations to these processes, and their subsequent influences upon the resolved-scale, are a primary source of forecast error. In this and the lectures to follow, our emphasis is on describing (1) the physics underlying the processes to be parameterized, (2) parameterization approaches for such processes, and (3) forecast sensitivity to chosen parameterization approaches for selected phenomena.

*An Introduction to Microphysical Parameterization*

Cloud microphysics refers to the set of physical processes controlling the formation of cloud droplets and ice crystals, their growth, and their fallout as precipitation. These processes act on the scales of cloud droplets and hydrometeors, with diameters on the order of micrometers ($10^{-6}$ m) to centimeters ($10^{-2}$ m). Consequently, these processes occur on scales well below those that are capable of being resolved by numerical weather prediction models (Fig. 1).

There are eight primary microphysical **species**: water vapor, cloud droplets, rain droplets, cloud ice crystals, snow, rimed ice, graupel, and hail. Microphysical parameterizations do not always include all of these species. For example, liquid microphysical parameterizations do not include frozen species; instead, they only include water vapor, cloud droplets, and rain droplets and the physical processes associated with their formation, growth, and decay.

In general, liquid microphysics are more straightforward to parameterize than frozen microphysical species. To first approximation, both cloud droplets and rain droplets are spheroids, and there are few physical processes that must be accounted for to accurately represent their formation, growth, and decay. Conversely, frozen species come in a wide range of shapes (or *habits*) and sizes and there are a litany of poorly understood physical processes that must be accounted for to accurately represent their formation, growth, and decay.

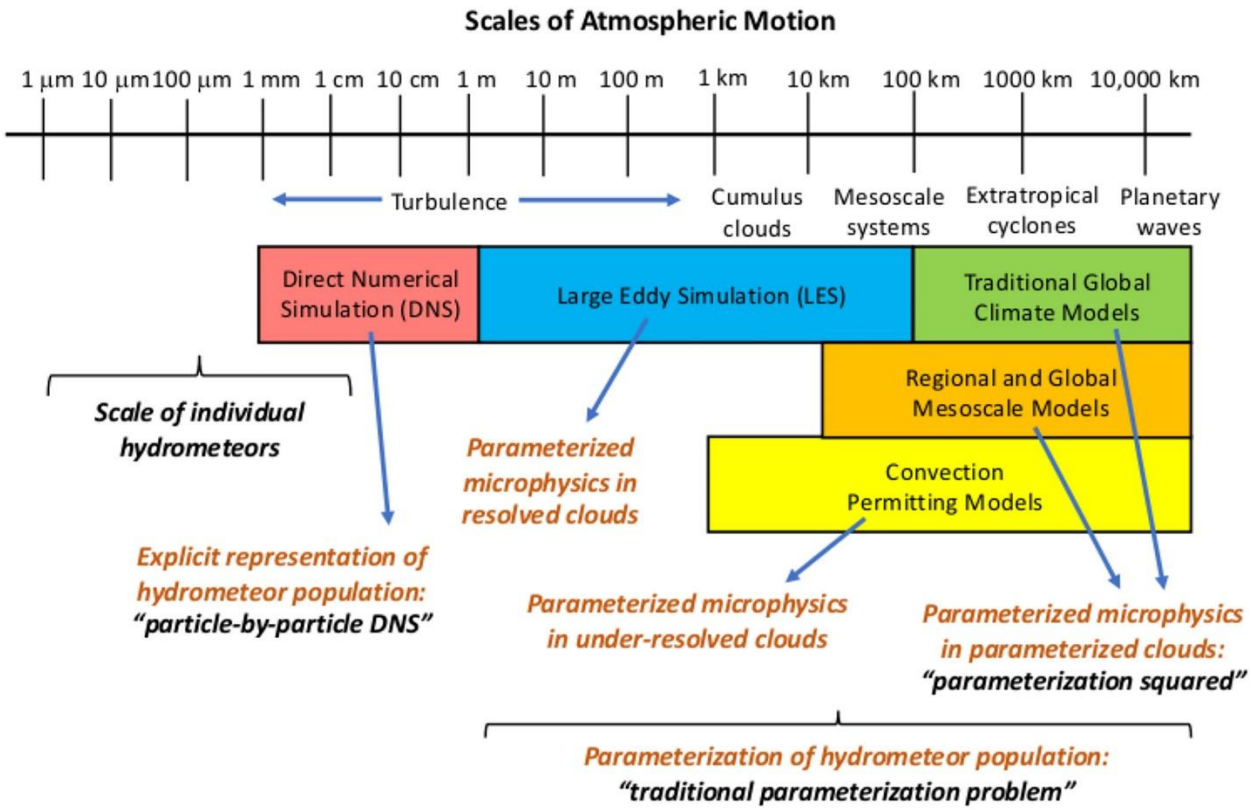


**Figure 1**. Schematic representation of atmospheric scales of motion, ranging from those of planetary waves on the far right to individual hydrometeors on the far left; the types of numerical models which typically represent or resolve those scales of motion (colored boxes); and how clouds and microphysics are handled in those models (orange and black text). Figure obtained from Morrison et al. (2020), their Fig. 2.

Typically, frozen species are treated by microphysical parameterizations as distinct species, each with underlying assumptions for particle density, total number concentration, and fall speed. This need not be the case, however, since the atmosphere is characterized by a wide range of frozen particles that have properties of multiple frozen species. Recently, microphysical parameterizations have been developed that predict specific properties, rather than species type, of frozen particles. These are typically formulated as functions of vapor deposition and riming rates since these rates are those which most effectively distinguish between frozen particle types (e.g., vapor deposition is dominant for ice crystals and snow whereas riming is dominant for rimed ice, graupel, and hail).

There are three classes of microphysical parameterizations, distinguished by how they represent the ***size distribution*** (relating total number concentration per unit volume to a particle's size) for microphysical species: **bulk**, **bin,** and **Lagrangian** (Fig. 2).

Bin microphysics parameterizations discretize the particle diameter size distribution into many bins. For each bin, predictive equations exist for the total number concentration per unit volume of each microphysical species. Changes in the total number concentration per unit volume may result from conversions between microphysical species or from particle growth and shrinkage. The existence of many bins and many predictive equations makes bin parameterizations computationally expensive relative to their bulk counterparts.

Lagrangian microphysics parameterizations represent the particle size distribution by "super particles," each representing a larger collection of particles for a given species, which follow trajectories in the modeled flow. As compared to bin and bulk parameterizations, which act in individual model grid columns and are thus Eulerian in formulation, Lagrangian parameterizations track species following the temporally evolving three-dimensional flow. However, a large number of "super particles" are needed to adequately represent the billions (or more) of microphysical particles within a model domain, rendering Lagrangian parameterizations very computationally expensive.

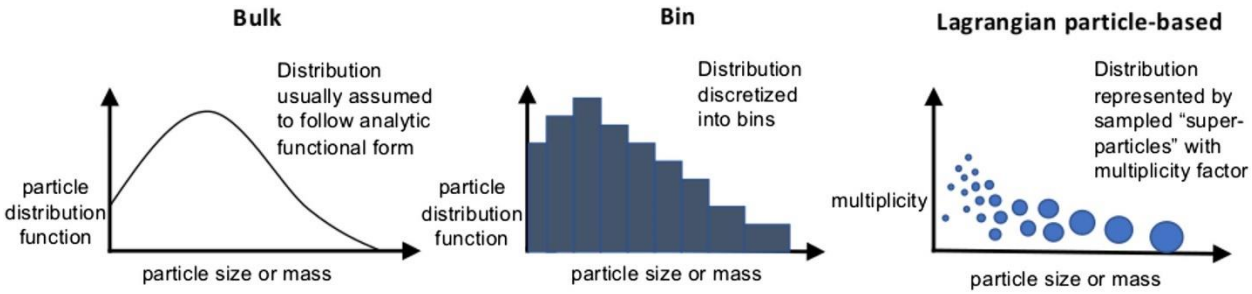


**Figure 2**. Schematic of a hypothetical size distribution, relating particle size or mass (*x*-axis) to the particle distribution function (representing the total number concentration per unit volume or mass) or multiplicity (representing the total number of particles for each particle size or mass) on the *y*-axis for (left) bulk, (center) bin, and (right) Lagrangian microphysical parameterizations. The different circle sizes in the right panel scale with particle size or mass. Figure obtained from Morrison et al. (2020), their Fig. 3.

Bulk microphysical parameterizations assume a prescribed analytic form for the size distribution of each microphysical species. This makes them less computationally expensive, and thus more widely used, than bin and Lagrangian parameterizations. The two most common analytic forms for the size distribution are the *inverse exponential* and *gamma* distributions. The former is a special case of the latter. The generic form of the gamma distribution is given by:

$$N(D) = N_0 D^{\mu} e^{-\lambda D}$$

Here, $N(D)$ is total number concentration per unit volume (units: $m^{-3}$), $D$ is particle diameter, $N_0$ is the intercept parameter that defines the maximum $N$ for a diameter of 0, $\mu$ is a shape parameter, and $\lambda$ is a slope parameter. The shape parameter can be related to the radar reflectivity factor $Z$, whereas the slope parameter can be related to the intercept parameter $N_0$ and mass mixing ratio $q$. The inverse exponential distribution arises for a shape parameter $\mu = 0$.

The gamma distribution has three free parameters: $\lambda$ ($q$, with a prescribed or diagnosed $N_0$), $N_0$, and $\mu$ ($Z$). Thus, there are three classes of bulk microphysical parameterizations:

- **Single-moment** parameterizations predict $\lambda$ which, with a diagnosed or fixed value of $N_0$, allows them to predict $q$.
- **Double-moment** parameterizations, which predict both $\lambda/q$ and $N_0$.
- **Triple-moment** parameterizations, which predict $\lambda/q$, $N_0$, and $\mu$ (and thus also $Z$).

Parameters that are not predicted by the microphysical parameterization are either *specified as constants* or are *empirically diagnosed from the predicted parameters*. Most widely used microphysical parameterizations are either single- or double-moment.

There are two primary benefits of double-moment versus single-moment parameterizations. First, predicting $N_0$ results in a more realistic particle-size distribution. Though this influences all particle types, this is of particular benefit to rain drops in the context of evaporation and hail in the context of melting. Focusing on the former for this discussion, single-moment schemes that fix $N_0$ for rain drops tend to predict unrealistically high counts of small-sized drops. Smaller drops have a greater ratio of surface area to volume (i.e., a greater fraction of the drop is in contact with the subsaturated surroundings) and thus more readily evaporate, resulting in greater evaporative cooling. Second, double-moment parameterizations more realistically treat size-sorting, wherein larger particles appear preferentially at lower altitudes since larger particles fall faster. Single-moment schemes do not realistically represent this size dependence.

A parameterization need not be single-, double-, or triple-moment for all microphysical species; some species may be treated with a higher-order representation while others are treated with a lower-order representation (e.g., Fig. 3).

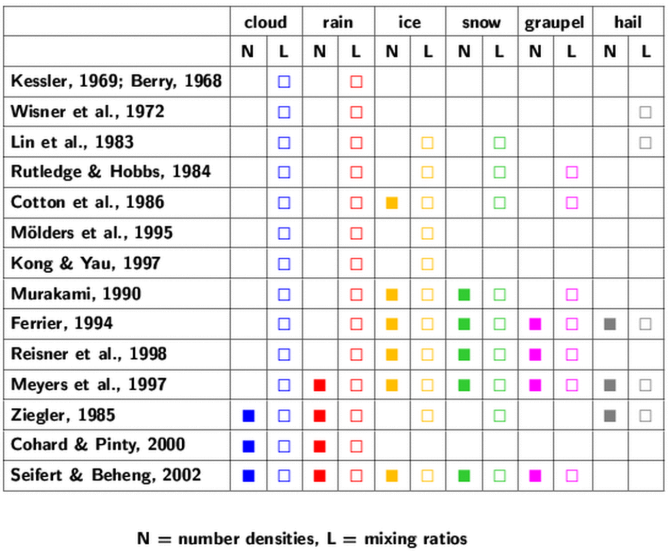


**Figure 3**. Microphysical species for which predictive equations exist for mixing ratio (open squares) and number concentration (filled squares) for selected microphysical parameterizations. Figure obtained from Seifert (2006), their Slide 10. Please see the WRF-ARW User's Guide section on microphysics for details regarding the parameterizations available in WRF-ARW.

Predictive equations for the mixing ratio of a generic species $q$ take the general form:

$$\frac{\partial q_x}{\partial t} = -\mathbf{v}\cdot\nabla q_x - \frac{1}{\rho_0}\nabla\left(\rho_0 \overline{\mathbf{v}' q_x'}\right) + \textit{conversion terms}$$

In the above, $q_x$ refers to the mixing ratio of any microphysical species (e.g., $q_v$ for water vapor, $q_r$ for rain droplets, $q_g$ for graupel, etc.) and $\rho_0$ is a constant base-state density. The first term on the right-hand side of this equation represents the three-dimensional advection of $q_x$. Note that for microphysical species with significant terminal velocities (all except vapor, cloud droplets, and cloud ice), there are two vertical advection terms: one for $w$ (or $\omega$) and one for the terminal velocity. The second term on the right-hand side of this equation represents the mean subgrid-scale turbulent mixing of $q_x$ and must be parameterized by the turbulence parameterization. The last term on the right-hand side of this equation is comprised of all relevant sources and sinks for $q_x$, described in more detail below.

In addition to predictive equations for the predicted moments, the effects of latent-heat release on the local temperature or potential-temperature tendency must also be included in a microphysical parameterization. These are functions of the relevant latent heats (of vaporization, of sublimation, etc.) and are not discussed further herein.

*Microphysical Species*

As noted above, there are eight primary microphysical species: water vapor, cloud droplets, rain, cloud ice, snow, rimed ice, graupel, and hail. We now wish to consider properties of each non-vapor species, including a discussion of the physical processes giving rise to each.

(1) Cloud droplets

Cloud droplets are liquid water droplets that form via the condensation of water vapor, primarily onto cloud condensation nuclei (CCN) when supersaturation is achieved. Cloud droplets range in size from ~$10^{-3}$ μm to ~100 μm. Their initial growth is primarily due to condensation and their initial rate of growth is inversely proportional to their size.

(2) Rain droplets

Rain droplets are liquid water droplets that form by the *collision and coalescence* of cloud droplets or by the melting of frozen hydrometeors. Rain droplets range in size from ~10 μm to ~1000 μm, with rain droplets' maximum size limited by droplet breakup resulting either from collisions with other droplets or aerodynamic drag. Collision and coalescence are most efficient when one droplet is of intermediate size (~30-50 μm) and the other droplet is ~30-85% of the size of the first. The physics behind this are threefold: a droplet that is too large is likely to breakup on colliding with another droplet; a droplet that is too small relative to another droplet is likely to flow around rather than collide with the larger droplet; and droplets that are of similar size to each other are unlikely to collide because of their similar fall velocities.

(3) Cloud ice crystals

Ice crystals are frozen water droplets that form by the homogeneous nucleation of liquid droplets at temperatures below -40°C (i.e., liquid water spontaneously freezing) or by ice nucleation onto ice nuclei (IN) at warmer temperatures, particularly at or below -10°C. There are four processes that result in ice nucleation:

- **Vapor deposition**: deposition of water vapor onto IN.
- **Condensation freezing**: condensation and freezing of water vapor onto IN.
- **Immersion freezing**: immersion of IN in supercooled water.
- **Contact freezing**: freezing of supercooled water upon contacting IN.

There are three primary types, or habits, of ice crystals: columns, dendrites, and plates. Temperature, the degree to which the atmosphere is supersaturated with respect to ice, and the means of ice nucleation all influence which habit is favored.

Ice crystals grow by vapor deposition in environments that are supersaturated with respect to ice. As this occurs, the environment becomes subsaturated with respect to water, resulting in the evaporation of supercooled water droplets and thus more available vapor that can be deposited onto the ice crystals. This is known as the Bergeron-Findeisen process.

(4) Snowflakes

Snowflakes result from the collision and coalescence, known as *aggregation*, of smaller ice crystals. As the efficiency of the aggregation process is a function of the complex shapes of the ice crystals involved, which is not readily observed, aggregation is a leading source of uncertainty in microphysical parameterizations.

(5) Rimed ice, graupel, and hail

Riming occurs as ice crystals collide and coalesce with supercooled cloud droplets at temperatures below 0°C. So long as the features of the original ice particle (e.g., crystal, snowflake) can be distinguished, the resulting ice particle is known as rimed ice. Once this is no longer true, the resulting ice particle is known as graupel. Contact-freezing nucleation is also an efficient means by which graupel may be generated. Graupel particles serve as embryos for hailstones, which require intense updrafts to form. Hail growth by riming may be "dry," wherein collected supercooled cloud droplets freeze upon contact with the hail stone, or "wet," wherein only a fraction of supercooled cloud droplets freeze on contact with the hail stone and the remainder are lost by shedding or are incorporated into the hail stone's inner core.

*Parameterized Processes: Formation, Growth, and Decay*

There are a wide range of physical processes that must be represented by microphysical parameterizations, many of which are depicted in a general sense in Fig. 4 and for an idealized cumulonimbus cloud in Fig. 5. Here, we define ten of these processes, including the species that they impact and briefly how they may be parameterized. Since the specific means by which each process is parameterized varies between parameterizations, only a high-level discussion of their parameterization is provided. Further, we do not discuss every process that redistributes particles vertically within a column (such as size sorting), yet these also must be accurately parameterized.

It should also be noted that many outstanding issues exist regarding the accurate parameterization of microphysical processes, particularly ice-phase microphysics. Nucleation, shape specification and prediction, aggregation, breakup, and riming are particularly challenging.

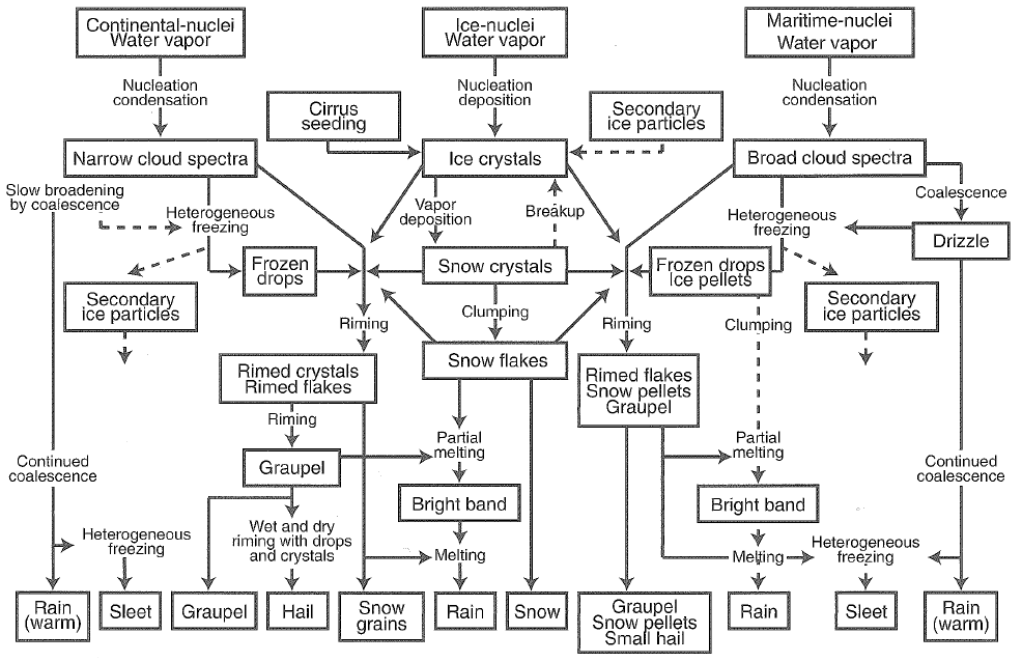


**Figure 4**. Schematic depicting the physical processes that are important for the formation of the precipitation types listed at the bottom of the figure. Note that not all microphysical processes, particularly those that do not lead to precipitation formation, are depicted. Figure reproduced from Warner (2011), their Fig. 4.2.

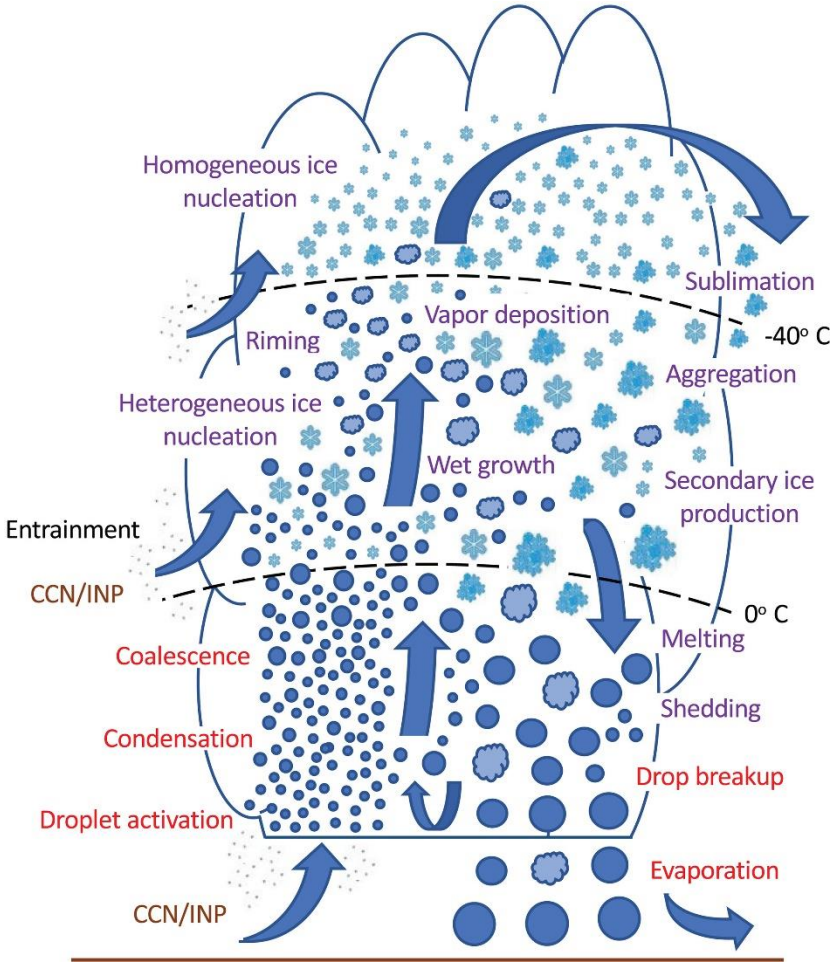


**Figure 5**. Schematic illustration of microphysical processes in an idealized cumulonimbus cloud. Red text indicates liquid-phase processes whereas purple text indicates ice-phase properties. Upward arrows, depicting upward motions in the cloud, generally correspond to processes leading to particle growth and suspension or lofting in the cloud. Downward arrows, depicting downward motions in the cloud, generally correspond to processes associated with particle fallout or shrinking and breakup. Figure reproduced from Morrison et al. (2020), their Fig. 1.

(1) Condensation

Most microphysical schemes assume that supersaturation with respect to liquid water is entirely offset by the condensation of many cloud drops. The amount of water vapor that is available to be condensed is equal to $q_v$ - $q_{vs}$, or the water-vapor mixing ratio minus the saturation water-vapor mixing ratio. Most of this water vapor condenses into cloud drops; however, the latent warming that accompanies condensation increases $q_{vs}$, in turn reducing the amount of condensation than if $q_{vs}$ remained constant.

Accurately representing the available CCN – e.g., such as may be provided by aerosol – is necessary to accurately parameterize condensation. The same is true for IN and ice initiation. Only in recent years has there been an effort to incorporate estimates of aerosol or CCN within microphysical parameterizations; however, climatological estimates are often used due to relatively few real-time aerosol and CCN observations.

(2) Autoconversion: collision and coalescence

Autoconversion is the process by which two cloud droplets collide and coalesce to form a larger cloud droplet or a smaller rain droplet. Autoconversion is generally parameterized as a function of the departure of the cloud-droplet mass (expressed in terms of the cloud-droplet mixing ratio $q_c$) or liquid water content from some threshold value.

(3) Accretion by liquid particles

Accretion is the process by which a rain drop (rather than a cloud droplet) collides and coalesces with a cloud droplet. It is typically parameterized as a function of the collection efficiency, rain drop content (often in terms of rain-water mixing ratio $q_r$), and cloud droplet content (often in terms of cloud-droplet mixing ratio $q_c$).

(4) Evaporation

Evaporation is typically parameterized as a complex function of temperature, thermal conductivity, the extent to which the air is subsaturated, and the diffusivity of water vapor in air. Viscous forces are also important. Evaporation results in latent cooling, which in turn lowers the saturation water-vapor mixing ratio, mitigating the extent to which evaporation can occur relative to an unchanged saturation water-vapor mixing ratio.

(5) Ice initiation

Most microphysical parameterizations assume that IN are activated to form ice crystals when the atmosphere is supersaturated with respect to ice. Thus, the ice-crystal concentration can be obtained given a known or assumed IN concentration. Knowing a typical ice crystal's mass allows for the ice-crystal concentration to be used to obtain the cloud ice mixing ratio $q_i$. Uncertainty abounds, however, in specifying the IN concentration as direct IN observations are typically unavailable.

(6) Aggregation by ice and snow crystals

Aggregation describes the growth of snow at the expense of ice crystals as they collide and coalesce with each other. It is most commonly parameterized as a function of the departure of the cloud ice mixing ratio from a threshold value; e.g., when sufficient cloud ice exists, some of it is said to aggregate and form snow.

(7) Accretion by frozen particles: riming

Accretion by frozen particles most commonly occurs as riming, or the accretion of cloud droplets and rain drops by graupel or snow to form larger graupel and/or hail. Cloud ice and snow may also be accreted, but their accretion is typically much less efficient than that of cloud droplets and rain drops. In either case, the parameterization of accretion is conceptually similar to that of accretion by liquid water, albeit with respect to the appropriate concentrations or mixing ratios.

(8) Deposition

Ice+crystal, snow, and graupel growth via deposition occur when the environment is supersaturated with respect to ice. Its parameterization is similar to that of evaporation and condensation, albeit necessitating modifications for the shape-dependent diffusivity of ice crystals.

(9) Melting

Falling ice particles gain heat from the environment, and thus begin to melt, by conduction and convection. Condensation, if the ice crystal is cooler than the environmental dewpoint, and evaporation, if the ice crystal is warmer than the environmental dewpoint, may accelerate or slow the melting rate, respectively. Melting rate is a function of temperature, although there exist slight differences in how this is specified (e.g., complete melting above 0°C versus only partial melting until the air temperature is several degrees above freezing).

(10) Sedimentation

Sedimentation represents the fallout of microphysical particles due to gravity. It typically only affects larger, heavier particles such as rain, snow, hail, and graupel, although it can affect smaller particles if in-cloud ascent is sufficiently weak.

Implicit to the parameterization of these processes are the assumed size distributions and, for ice phase processes, assumptions regarding ice crystal types and shapes.

This is not an exhaustive list of physical processes that must be parameterized by microphysical parameterizations. For example, not included within the above list is the breakup of both snow crystals and rain droplets due to aerodynamic drag as they fall. Indeed, breakup is a physical process for which limited understanding exists of its particulars, and consequently it is a large contributor to errors associated with microphysical parameterizations. Also not included is the fall speed of precipitating hydrometeors, which is dependent on hydrometeor size and mass and enters the extended vertical advection term for certain microphysical species.

The allowed interactions between species for selected microphysical parameterizations available with the WRF-ARW model are depicted in Fig. 6. Physical processes resulting in conversions between species and/or the growth of particles within a given species are depicted in Fig. 7. These are the processes that must be parameterized with a microphysical parameterization. The specifics of these processes vary, often significantly, between individual parameterizations.

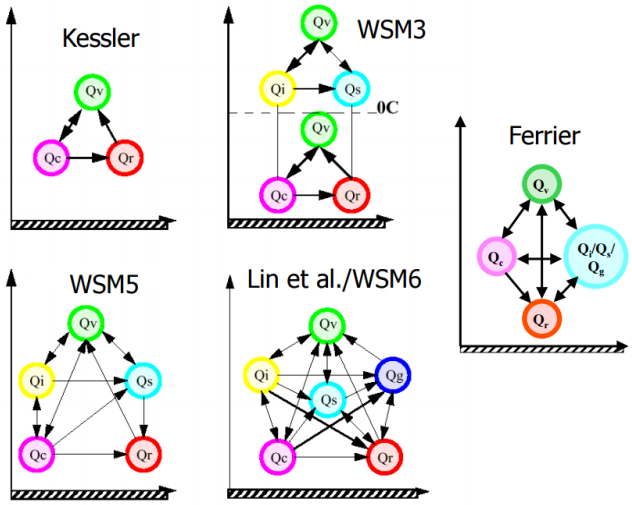


**Figure 6**. Illustration of the allowable conversions between microphysical species, in terms of their mixing ratios, for six single-moment bulk microphysical parameterizations available in WRF-ARW: Kessler, WRF Single Moment-3 Class (WSM3), Ferrier, WRF Single Moment-5 Class (WSM5), and the Lin et al. and WRF Single Moment-6 Class (WSM6) parameterizations. Subscripts refer to microphysical species: *v* for water vapor, *c* for cloud droplets, *r* for rain drops, *i* for cloud ice particles, *s* for snow, *g* for graupel. Figure obtained from Dudhia (2010), their Slide 3.

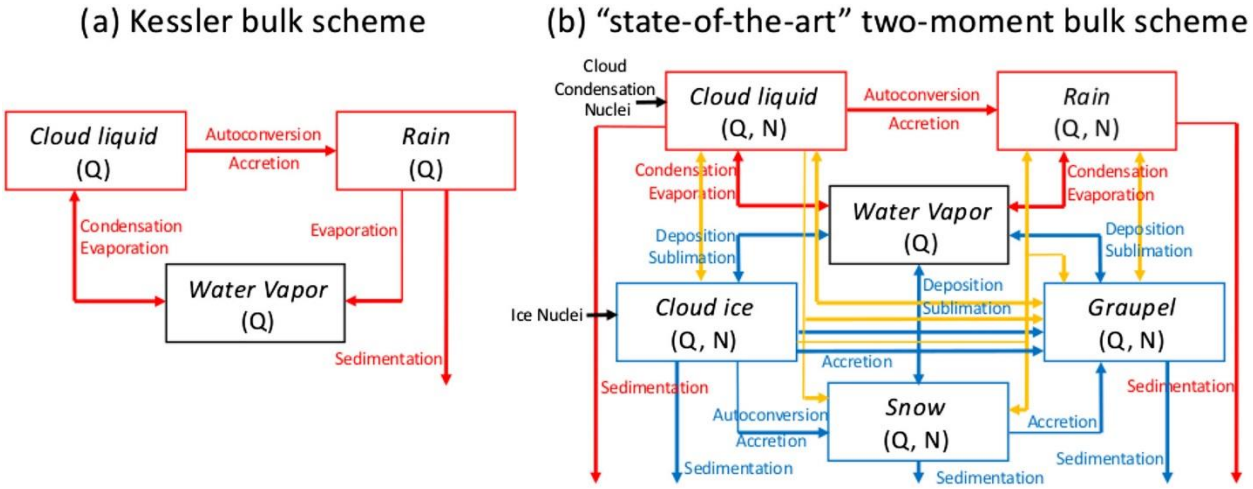


**Figure 7**. (a) Schematic indicating the cloud microphysical processes associated with conversions between water vapor, cloud droplets, and rain as parameterized by the Kessler "warm rain" microphysics parameterization. For example, evaporation can result in a gain of water vapor at the expense of raindrops and/or cloud droplets. (b) Schematic indicating the cloud microphysical processes associated with conversions between water vapor, cloud droplets, rain, cloud ice, graupel or hail, and snow as parameterized by most modern double-moment bulk microphysics parameterizations. Red, yellow, and blue arrows represent liquid, mixed-phase, and ice-phase processes, respectively. Figure obtained from Morrison et al. (2020), their Fig. 4.

Above, we stated that predictive equations for mixing ratio $q$ take the general form:

$$\frac{\partial q_x}{\partial t} = -\mathbf{v}\cdot\nabla q_x - \frac{1}{\rho_0}\nabla\left(\rho_0 \overline{\mathbf{v}' q_x'}\right) + \textit{conversion terms}$$

where *conversion terms* include all relevant sources and sinks for $q_x$. For water vapor ($q_v$), Fig. 7b indicates that water-vapor mass in realistic microphysical parameterizations is gained by the evaporation of cloud droplets and rain drops and by the sublimation of cloud ice crystals, snow, and graupel. Water-vapor mass is lost by condensation to cloud droplets and by deposition to cloud ice crystals, snow, and graupel. These processes and their effects on their environments, as well as those for all other microphysical species, must be parameterized.

For double- and triple-moment microphysical parameterizations, similar predictive equations exist for number concentration and reflectivity factor, respectively. For example, Appendix A of Milbrandt and Yau (2005, Part II, *J. Atmos. Sci.*) presents predictive equations for mixing ratio, number concentration, and reflectivity factor for all microphysical species represented in their parameterization. Section 7.4 of *Parameterization Schemes* provides similar details for a wide range of parameterizations.

*Other Considerations Relevant to Microphysical Parameterization*

Microphysical parameterizations do not act independent of other parameterizations (Fig. 8). The radiation budget is influenced by clouds, which reduce both incoming shortwave and outgoing longwave radiation. Non-convective precipitation from the microphysical parameterization can impact local soil-moisture content, and the relatively cool, moist conditions that accompany precipitation can influence surface heat and moisture fluxes. The detrainment of microphysical species in proximity to deep convective clouds parameterized by the cumulus convection parameterization can in turn influence the local microphysical tendencies.

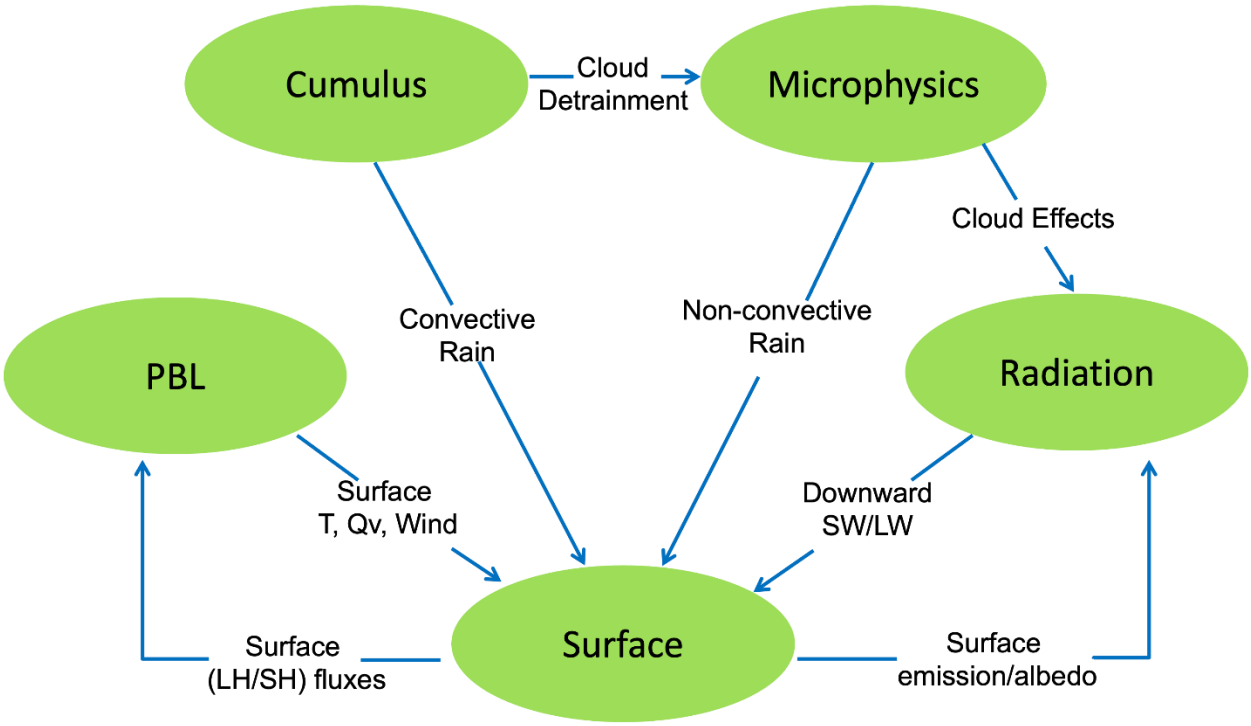


**Figure 8**. Illustration of the *direct* interactions that occur between physical parameterizations within a numerical model. While indirect interactions also exist, these are not depicted here for brevity. Figure obtained from the WRF-ARW User's Guide section on WRF Physics.

Direct observations of microphysical species are not routinely available. Yet, we often desire that a numerical model contains realistic precipitating phenomena at its initialization time, as in a "hot start" initialization. This requires accurately specifying all prognostic microphysical variables during the initialization process, which itself requires data assimilation. Accurately specifying all prognostic microphysical variables via data assimilation is an area of active research, with dual-polarization Doppler radar and disdrometer data offering promise in this

regard. However, assimilating radar data poses a significant challenge for most existing data-assimilation systems, primarily with respect to adjusting model variables (e.g., temperature, pressure, wind) from the assimilated data. An alternative approach used with "cold start" initializations is to have all microphysical variables except water-vapor mixing ratio be zero at the simulation's outset. In this approach, the model must "spin up" the other variables, a process that can take several hours to successfully complete.

In recent years, double-moment microphysical parameterizations have gained more widespread acceptance. This has largely been driven by increases in computer power and a desire to represent microphysical processes and their resolved-scale impacts more realistically in model forecasts. However, this does not guarantee improved forecasts owing primarily to atmospheric non-linearity. More realistically treating microphysical processes may expose other model shortcomings that were previously hidden. Further, since other parameterizations may have been developed and/or tuned to work with simpler schemes, degraded skill may result when they are used with more-complex parameterizations – even if the inputs from these parameterizations are improved!

*Practical Examples of Forecast Sensitivity to Microphysical Parameterization*

There are many published works in which the forecast sensitivity for precipitating phenomena such as supercells, continental and tropical mesoscale convective systems, winter storms, and so on, to microphysical parameterization has been evaluated. Here, we consider a subset of these works, focusing on a single example for many of the phenomena above.

The results of these studies are likely somewhat generalizable over a wider range of cases than those reported on in a given manuscript. However, keep in mind that the results presented in these manuscripts are formally valid only for the cases and conditions considered within the given study.

(1) **Supercells**: Gilmore et al. (2004, *Mon. Wea. Rev.*)

Idealized simulations of supercells under a range of vertical wind shear magnitudes were conducted using three microphysical parameterizations, two that are liquid-only and one that includes frozen species.

Phase changes to and from ice species are associated with latent heat release. Recall that the latent heat of melting is much larger than the latent heat of vaporization, and the latent heat of sublimation is larger yet. Consequently, latent warming and cooling associated with phase changes to and from ice species, respectively, are much greater than if only liquid species are represented.

The latent heat release that occurs in a convective updraft as vapor deposits or liquid water freezes increases the updraft's buoyancy and thus its intensity. This slows the rate of ice-crystal fallout, in turn slowing the rate of precipitation production. It also promotes greater condensate, formed by lifting subsaturated air parcels to saturation, and more precipitation (Fig. 9).

Latent cooling in a convective downdraft due to melting or sublimation results in stronger surface cold pools, although similar results can be achieved if evaporation in a liquid-only parameterization is sufficiently strong. This also influences the cold pool's areal extent and the lifting magnitude along its leading edge, in turn affecting the baroclinically generated horizontal vorticity and storm structure.

Though illustrative of tenets related to liquid versus ice microphysics, note that this study should not be taken as an example of the extent to which supercell simulations are sensitive to variations between modern microphysics parameterizations (e.g., single- versus double- moment schemes).

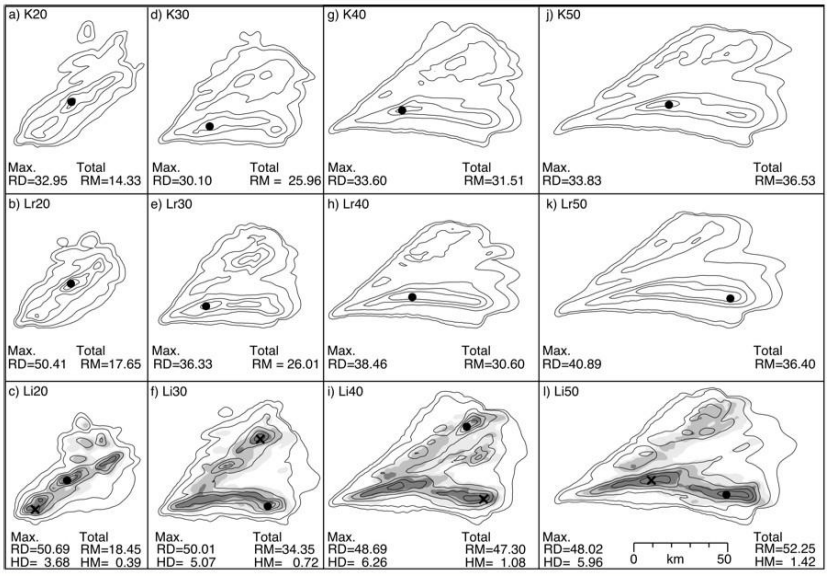


**Figure 9**. 2-h accumulated rainfall (mm; contoured at 0.1, 1, 10, 20, 30, 40, and 50 mm) and hail/graupel (mm; shaded at 0.01, 0.1, and 1 mm) for simulations of an idealized supercell conducted using the (a, d, g, j) Kessler liquid-only, (b, e, h, k) Lin liquid-only, and (c, f, i, l) Lin full microphysical parameterizations. Panels (a-c), (d-f), (g-i), and (j-l) depict simulation output for cases with 20, 30, 40, and 50 m $s^{-1}$ of 0-5 km vertical wind shear, respectively. RD and HD denote the maximum rain and hail depths (mm), respectively, while RM and HM denote the total accumulated mass (in Teragrams) of rain and hail, respectively. Figure obtained from Gilmore et al. (2004), their Fig. 12.

(2) **Supercells**: Dawson et al. (2015, *Mon. Wea. Rev.*)

Four high-resolution ($\Delta x$ = 1 km) simulations, differing in only the number of moments for which the Milbrandt & Yau microphysical parameterization contains predictive equations, were conducted of the 3 May 1999 Moore, OK tornadic supercell. The single-moment version of the parameterization only predicts mixing ratio, the double-moment version also predicts the intercept parameter $N_0$, and the triple-moment version also predicts the shape parameter $\mu$ and thus the reflectivity factor $Z$.

The single-moment-based simulations predicted a supercell cold pool that is too cold, with a low-level updraft tilt rearward with height that is too large and thus a mesocyclone that is too weak, relative to both the double- and triple-moment-based simulations and to observations (Fig. 10). The single-moment simulation also predicts significantly more rain-drop evaporation of rain drops than do its counterparts (Fig. 11).

These simulation variations result from the treatment of the intercept parameter, which is held fixed in the single-moment simulation and predicted or variable in the double- and triple-moment simulations. As rain drops evaporate, the size distribution must change shape because the number concentration must go down. Because of the larger ratio between the surface area and drop volume, smaller rain drops evaporate more readily than do larger rain drops, and so the size distribution *should* reduce number concentrations at smaller diameters. This is what occurs in the double- and triple-moment simulations.

In the single-moment simulation, however, the intercept parameter that specifies the number concentration at $D = 0$ is fixed (i.e., there is a constant number of infinitesimally small rain drops), and thus the greatest change in the size distribution is non-physical – with larger rain drops. This, in turn, promotes even more evaporation of the small drops that remain! While the single-moment simulation also predicts greater raindrop mass (for reasons that are not immediately obvious), this study shows that it is the treatment of raindrop evaporation for a fixed mass that exerts the greatest influence on the forecast.

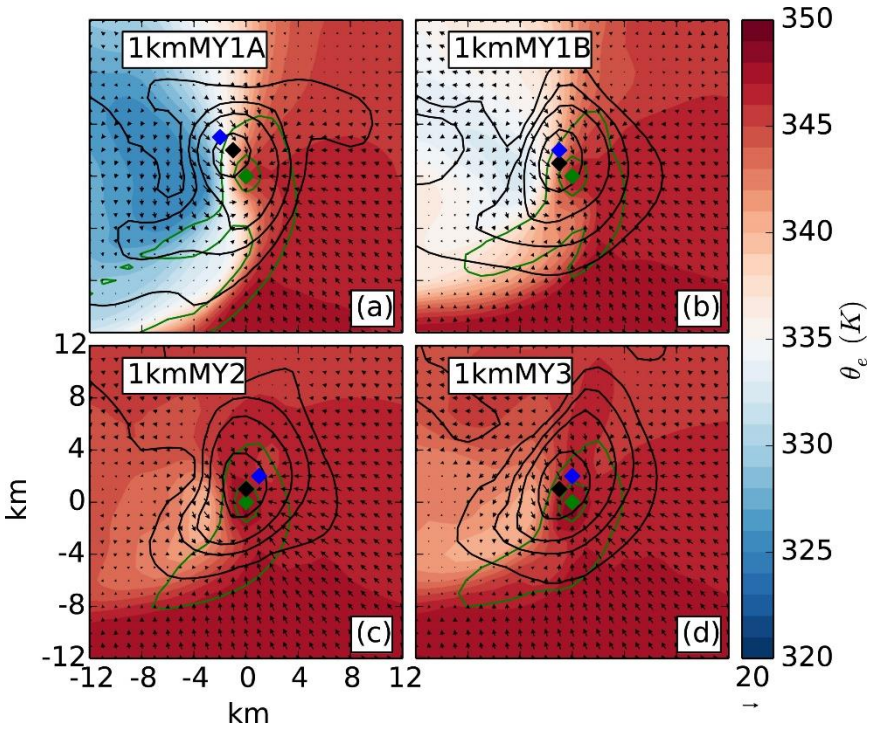


**Figure 10**. 1.5-hour storm-centered composites of surface equivalent potential temperature ($\theta_e$; shaded in K), surface winds (vectors; reference vector in m $s^{-1}$ at lower right), 186-m AGL vertical velocity (green contours at 0.5 and 2.5 m $s^{-1}$), 3.1-km AGL vertical velocity (black contours at 1, 5, 10, and 20 m $s^{-1}$), and updraft centers at 186-m (black), 3.1-km (green), and 6.1-km (blue) from the (a) single-moment, (b) single-moment with a reduced $N_0$, (c) double-moment, and (d) triple-moment simulations of Dawson et al. (2015). Figure reproduced from their Fig. 9.

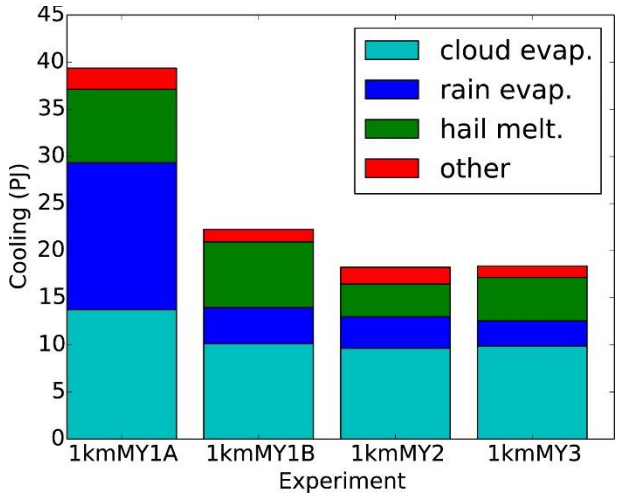


**Figure 11**. Temporally (over a 1.5-h period) and spatially (in 48 x 48 km$^2$ boxes following the low-level mesocyclone, below 4 km AGL, and within downdraft regions only) integrated latent cooling (petajoules, or PJ) due to cloud droplet evaporation (teal), rain drop evaporation (blue), hail melting (green), and other processes (red) from the single-moment (1kmMY1A), single-moment with a reduced $N_0$ (1kmMY1B), double-moment (1kmMY2), and triple-moment (1kmMY3) simulations of Dawson et al. (2015). Figure reproduced from their Fig. 12.

(3) **Tropical mesoscale convective systems**: van Weverberg et al. (2013, *J. Atmos. Sci.*)

Three simulations, differing only by their microphysical parameterization, were conducted of a series of mesoscale convective systems in the tropical Pacific Ocean. Differences between the simulations primarily manifest with respect to the sedimentation of ice particles aloft. When sedimentation was slower to occur, more frozen condensate (snow and graupel; Fig. 12) formed and more expansive anvils resulted. This resulted more from differences in ice particle number concentrations than from differences in parameterized fall speeds (e.g., for both, varying the number of large ice crystals aloft).

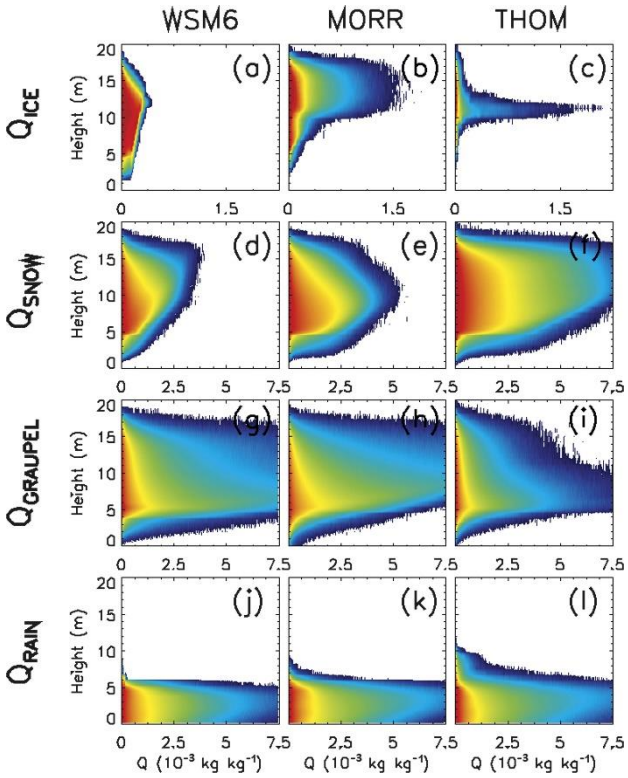


**Figure 12**. Contoured frequency by altitude, aggregated hourly over the entire analysis domain, of (a-c) cloud ice mixing ratio, (d-f) snow mixing ratio, (g-i) graupel mixing ratio, and (j-l) rain water mixing ratio for the (a, d, g, j) WSM6, (b, e, h, k) Morrison, and (c, f, i, l) Thompson schemes. The units of mixing ratio are g $kg^{-1}$; the units of altitude are km. Shading denotes the frequency of occurrence, with warmer colors indicate more-frequent occurrences and colder colors indicating less-frequent occurrences. Figure obtained from van Weverberg et al. (2013), their Fig. 8.

(4) **Lake-effect snow**: Reeves and Dawson (2013, *J. Appl. Meteor. Climatol.*)

Eight simulations, differing only with respect to their microphysical parameterizations, were conducted of a lake-effect snow event. Two precipitation regimes were identified: steady, characterized by relatively broad and uniform precipitation shields, and unsteady, characterized by relatively narrow precipitation shields with more localized maxima (Fig. 13). Hydrometeors remained in-cloud longer for steady versus unsteady cases.

Differences between schemes resulted from (a) the treatment of graupel production via the accretion of snow by rain drops, with more graupel production in the unsteady cases, and (b) the dependence of fall speed on riming intensity. The former applies to schemes that include graupel, whereas the latter applies to schemes that include graupel. A lack of

observations of these processes during lake-effect snow events precludes identifying a 'best' scheme.

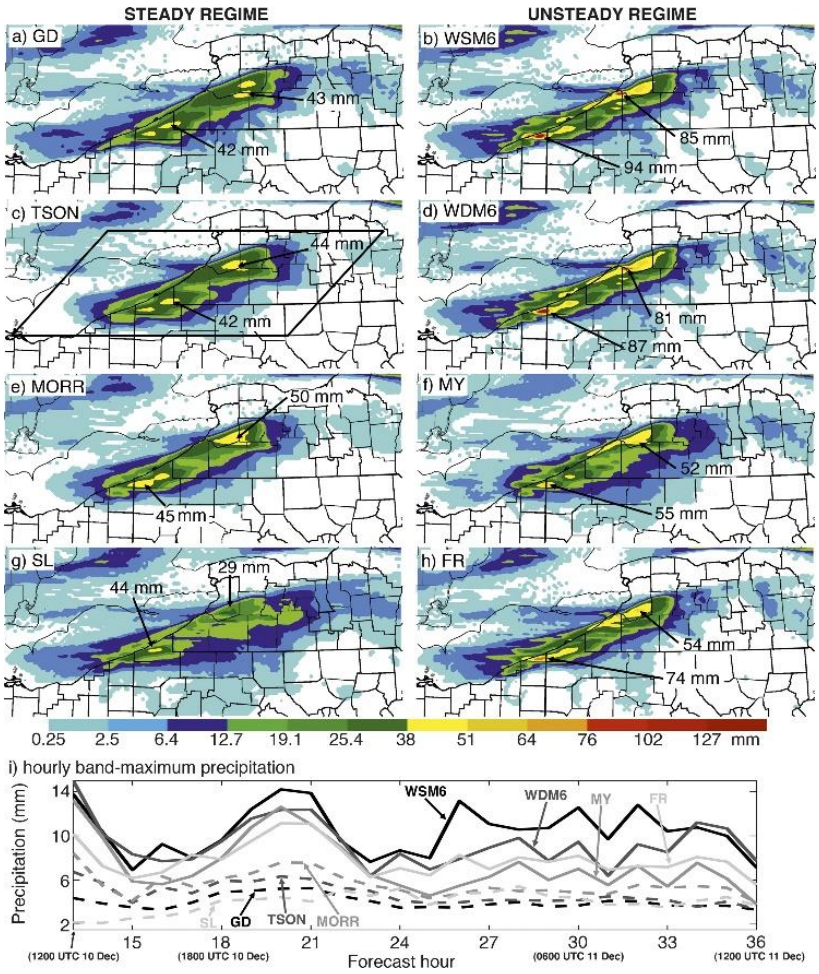


**Figure 13**. Accumulated precipitation (mm) between 12-36 h for the (a) Goddard, (b) WSM6, (c) Thompson, (d) WDM6, (e) Morrison, (f) Milbrandt and Yau, (g) Stony Brook, and (h) Ferrier microphysical parameterizations. In panel (i), the maximum hourly precipitation anywhere within the lake-effect band is plotted for each of the eight simulations. Figure obtained from Reeves and Dawson (2013), their Fig. 3.

(5) **Orographic snow**: Liu et al. (2011, *Mon. Wea. Rev.*)

Orographically forced snow events in the Colorado mountains, nominally associated with relatively weak (< 2 m $s^{-1}$) ascent, were simulated using seven different microphysical parameterizations. Forecast skill for precipitation was a function of cloud water and

graupel content. The most skillful forecasts, here produced by the Thompson and Morrison microphysics schemes, were associated with more cloud water and less graupel (Fig. 14). These differences resulted from different treatments of ice initiation, graupel formation and growth, and the fall speed of snow between the considered parameterizations.

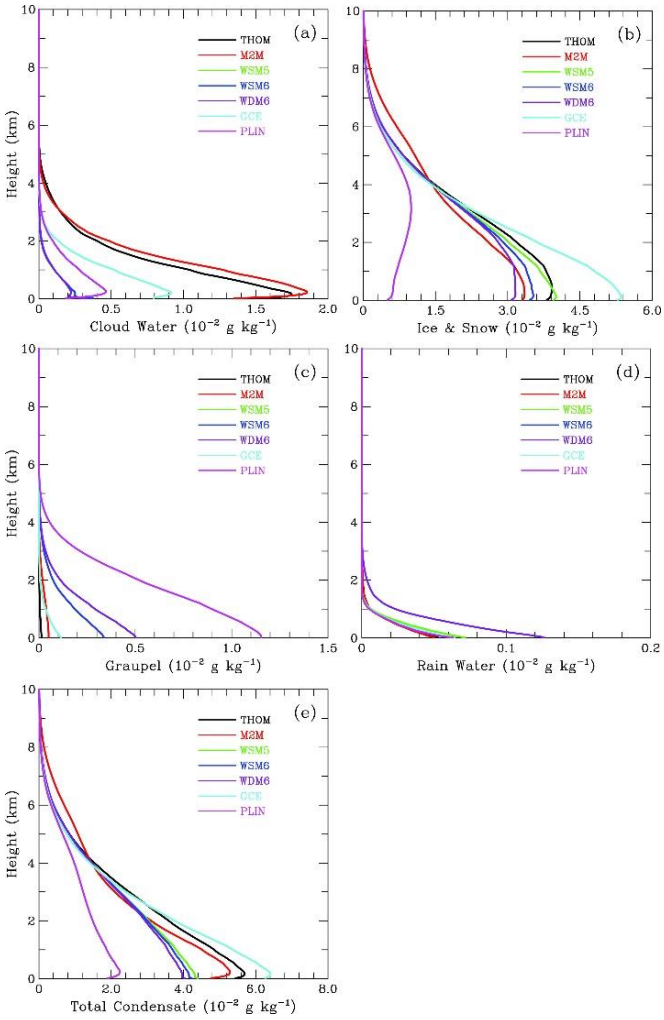


**Figure 14**. Spatially and temporally averaged vertical profiles of (a) cloud-water mixing ratio, (b) cloud ice + snow mixing ratio, (c) graupel mixing ratio, (d) rain-water mixing ratio, and (e) total mixing ratio. All fields have units of $10^{-2}$ g kg$^{-1}$. Outputs from the Thompson, Morrison, WSM5, WSM6, WDM6, Goddard, and Lin microphysical parameterizations are depicted by the black, red, green, dark blue, dark purple, light blue, and light purple lines, respectively. Figure obtained from Liu et al. (2011), their Fig. 10.

(6) **Atmospheric rivers**: Jankov et al. (2009, *J. Hydrometeor.*)

Significant differences between microphysical schemes with respect to their partitioning of water condensate were identified in simulations of five cool-season atmospheric river events in the western United States (Fig. 15), particularly with respect to cloud drops versus cloud ice and snow versus graupel. Though no effort was made to determine the cause of these differences, it can be inferred that they result from the varying treatments for the treatment of larger ice particles (e.g., growth of snow versus growth of graupel) and ice versus condensation nucleation.

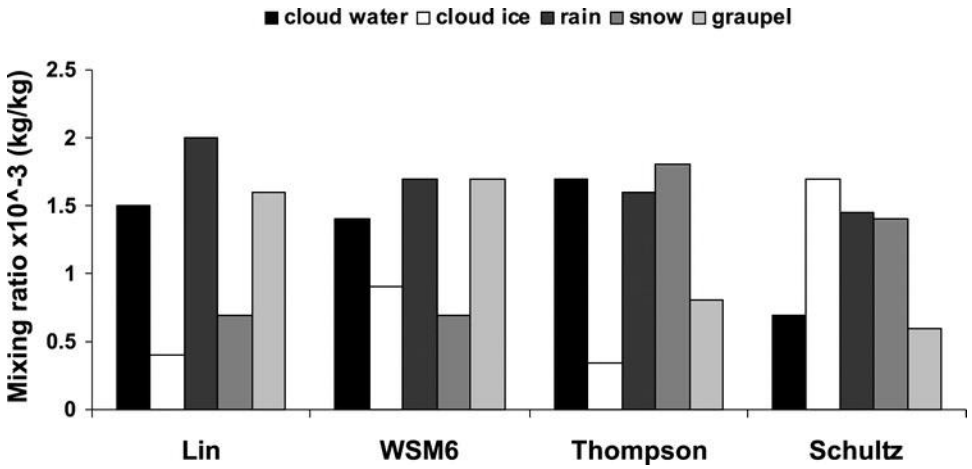


**Figure 15**. Volume-integrated cloud water, cloud ice, rain, snow, and graupel mixing ratios (g $kg^{-1}$), averaged over five numerical simulations of atmospheric river events in the western United States, conducted using four different microphysical parameterizations (Lin, WSM6, Thompson, and Schultz). Figure obtained from Jankov et al. (2009), their Fig. 8.